Mn2(2,5-disulfhydrylbenzene-1,4-dicarboxylate): A Microporous Metal–Organic Framework with Infinite (–Mn–S–)∞ Chains and High Intrinsic Charge Mobility

ARTICLE *in* JOURNAL OF THE AMERICAN CHEMICAL SOCIETY · MAY 2013

Impact Factor: 12.11 · DOI: 10.1021/ja4037516

4 AUTHORS, INCLUDING:

Lei Sun
Massachusetts Institute of Technology
13 PUBLICATIONS **201** CITATIONS
SEE PROFILE

Shu Seki
Kyoto University
403 PUBLICATIONS **6,695** CITATIONS
SEE PROFILE

JACS
JOURNAL OF THE AMERICAN CHEMICAL SOCIETY

Communication

pubs.acs.org/JACS

Mn_2(2,5-disulfhydrylbenzene-1,4-dicarboxylate): A Microporous Metal−Organic Framework with Infinite $(-Mn-S-)_\infty$ Chains and High Intrinsic Charge Mobility

Lei Sun,[†] Tomoyo Miyakai,[‡] Shu Seki,[‡] and Mircea Dincă*[,†]

[†]Department of Chemistry, Massachusetts Institute of Technology, 77 Massachusetts Avenue, Cambridge, Massachusetts 02139, United States

[‡]Department of Applied Chemistry, Graduate School of Engineering, Osaka University, Suita, Osaka 565-0871, Japan

Supporting Information

ABSTRACT: The reaction of $MnCl_2$ with 2,5-disulfhydrylbenzene-1,4-dicarboxylic acid (H_4DSBDC), in which the phenol groups in 2,5-dihydroxybenzene-1,4-dicarboxylic acid (H_4DOBDC) have been replaced by thiophenol units, led to the isolation of Mn_2(DSBDC), a thiolated analogue of the M_2(DOBDC) series of metal−organic frameworks (MOFs). The sulfur atoms participate in infinite one-dimensional Mn−S chains, and Mn_2(DSBDC) shows a high surface area and high charge mobility similar to that found in some of the most common organic semiconductors. The synthetic approach to Mn_2(DSBDC) and its excellent electronic properties provide a blueprint for a potentially rich area of exploration in microporous conductive MOFs with low-dimensional charge transport pathways.

Myriad applications have been found or proposed for microporous metal−organic frameworks (MOFs),[1] yet those that require electron transport or conductivity in combination with permanent porosity still lag behind because the vast majority of microporous MOFs are electrical insulators.[2] However, recent inroads in this area have suggested that judicious choice of the metal and organic components can lead to crystalline porous materials with promising conductivity or charge mobility properties.[3] In fact, taking a cue from the more mature area of molecular conductors and conductive coordination polymers, one can envision that two main approaches can be employed to construct new MOFs with good charge transport properties.[4,5] One is the "through-space" approach, which relies on π-stacking interactions between electroactive moieties. This approach has led to remarkable results with covalent organic frameworks[6] and has also recently been used by us to make a tetrathiafulvalene (TTF)-based MOF with high charge mobility.[3c] The second approach relies on a "through-bond" formalism, where both symmetry and energy overlap between the covalently bonded components must exist to promote good charge transport. This approach is synthetically more tractable because it allows control of the directionality of the metal−ligand bond. It has nevertheless seen limited success in MOFs, which are typically constructed from hard metal ions and oxygen- or nitrogen-based redox-inactive ligands[7] that rarely provide a good pathway for charge delocalization. Replacement of oxygen atoms by sulfur can alleviate the energy mismatch[8] and has led to semiconducting nonporous coordination polymers[9] and one of the only examples of a porous and conductive material, a Ni−dithiolene MOF.[3a] We sought to pursue a related approach in which the oxygen atoms in metal−oxygen chains of existing MOFs are replaced isomorphically by sulfur atoms, thereby giving rise to infinite metal−sulfur chains of potential interest in regard to charge transport. In essence, this approach would create dimensionally reduced metal−organic chalcogenides wherein the organic spacers would create porosity while maintaining $(-M-S-)_\infty$ units along one direction. Although theoretical and experimental studies have indicated that dimensional reduction in bulk metal chalcogenides (which are usually intrinsic semiconductors or metals[10]) increases the band gap of these materials, the lower dimensionality does not eliminate charge transport.[11]

There are numerous MOFs that contain infinite one-dimensional (1D) secondary building units (SBUs) in which single oxygen atoms bridge pairs of metal ions. One of the most iconic examples is the series of materials with the formula M_2(DOBDC) (M = Mg, Mn, Fe, Co, Ni, Zn; H_4DOBDC = 2,5-dihydroxybenzene-1,4-dicarboxylic acid).[12] The SBUs in these MOFs are $(-M-O-)_\infty$ chains where each pair of metal atoms is bridged by one phenolate group. We surmised that replacing the phenol groups by thiophenol functionalities would give rise to isomorphous materials with linear $(-M-S-)_\infty$ units and high charge mobility (Figure 1). Herein we show that 2,5-disulfhydrylbenzene-1,4-dicarboxylic acid (H_4DSBDC), the thiolated analogue of H_4DOBDC, generates Mn_2(DSBDC), a new material with permanent porosity and high charge mobility. To our knowledge, the new MOF has the highest surface area among MOFs that display electron delocalization, improving the previous record by almost 50% and reinforcing the idea that high surface area and charge delocalization can indeed coexist in crystalline hybrid materials.

The ligand precursor H_4DSBDC was synthesized starting from hydroquinone in five steps and 19% overall yield according to Scheme S1 in the Supporting Information (SI).[13] Heating a solution of H_4DSBDC and anhydrous $MnCl_2$ in a dry and degassed mixture of *N*,*N*-dimethylformamide (DMF) and methanol (10:1 by volume) at 120 °C under a nitrogen

Received: April 15, 2013
Published: May 14, 2013

dx.doi.org/10.1021/ja4037516 | J. Am. Chem. Soc. 2013, 135, 8185−8188

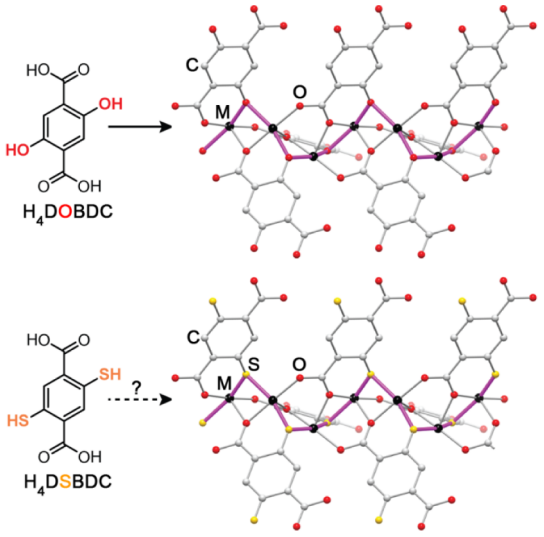

Figure 1. Conceptual design of MOFs containing $(-M-S-)_\infty$ chains obtained by replacing phenol groups in M_2(DOBDC) with thiophenol groups. The purple bonds indicate the infinite $(-M-O-)_\infty$ chains in M_2(DOBDC) and the expected $(-M-S-)_\infty$ chains in M_2(DSBDC).

atmosphere for 1 day generated yellow crystals of $[Mn_2(DSBDC)(DMF)_2]\cdot 0.2DMF$ (as-synthesized **1**) and an unidentified orange powder. Single-crystal X-ray diffraction (XRD) analysis of **1** revealed a structure consisting of infinite Mn^{2+} chains bridged by both carboxylate groups and thiophenoxide groups of anionic $DSBDC^{4-}$ ligands (Figure 2). Although related to the structure of M_2(DOBDC), the structure of **1** is different because two crystallographically independent Mn^{2+} ions are found in the asymmetric unit, whereas only one is present in M_2(DOBDC). In **1**, one Mn^{2+} ion is coordinated by four carboxylate oxygen atoms and two thiophenoxide groups, while another is coordinated by two carboxylate oxygen atoms, two thiophenoxide groups and two cis-oriented DMF molecules. Importantly, **1** contains infinite $(-Mn-S-)_\infty$ chains defined by Mn^{2+}–thiophenoxide linkages wherein the sulfur atoms at both crystallographic Mn sites are oriented trans to each other, with Mn–S distances of 2.493(1) and 2.632(1) Å, respectively. This indicates that the S atoms interact with the same d orbital of Mn, an important symmetry requirement for charge delocalization along the $(-Mn-S-)_\infty$ chain. Bridging in each pair of neighboring Mn atoms is completed by one oxygen atom from carboxylate groups and μ-carboxylate linkages. Neighboring chains are connected by $DSBDC^{4-}$ ligands that together define a three-dimensional framework containing hexagonal 1D pores with a van der Waals diameter of ~16 Å (for fully activated **1**). As expected on the basis of the longer Mn–S and C–S distances relative to M–O and C–O, respectively, this is ~2.4 Å larger than that found in M_2(DOBDC) analogues[12c] and is much larger than those found in previous conductive MOFs,[3] suggesting potential applications in donor–acceptor studies.

Attempts to eliminate the unidentified secondary orange product led us to increase the methanol content of the solvent mixture. Although gradually increasing the methanol content visibly decreased the amount of undesired orange product, it also decreased the crystal size of **1**. Pure **1** was obtained as a microcrystalline yellow material when the DMF/methanol ratio reached 2:1. Its identity and purity were verified by powder XRD (PXRD), which revealed a pattern corresponding to that simulated from the single-crystal X-ray structure (Figure 3).

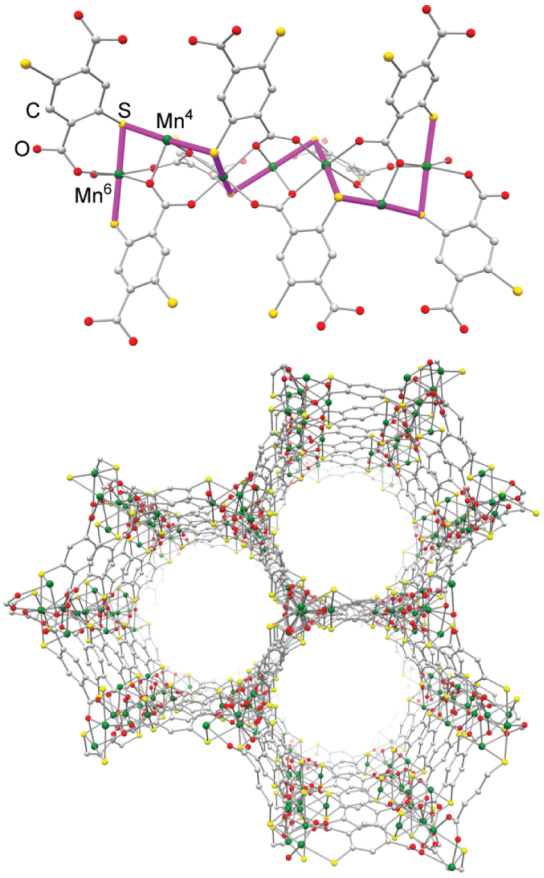

Figure 2. Portions of the X-ray crystal stucture of Mn_2(DSBDC). (top) View of an $(-M-S-)_\infty$ chain SBU. Mn^4 and Mn^6 represent fourfold- and sixfold-coordinated Mn sites, respectively, in activated Mn_2(DSBDC). (bottom) View of infinite 1D pores along the *c* axis. H atoms and DMF molecules have been omitted for clarity.

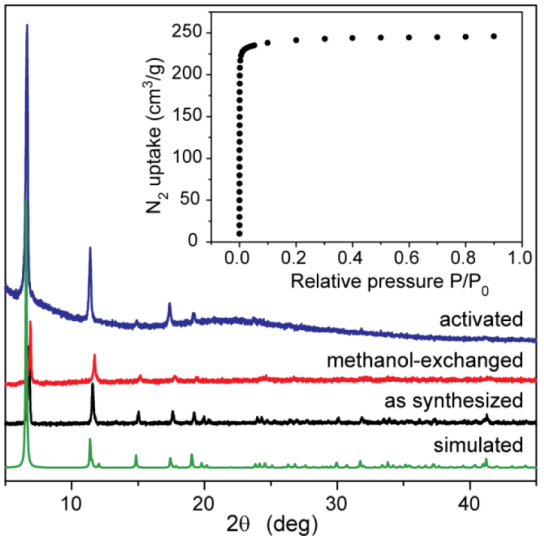

Figure 3. PXRD patterns of as-synthesized **1**, methanol-exchanged **1**, and activated **1** and the simulated pattern obtained from the single-crystal X-ray structure of **1**. The inset shows the N_2 adsorption isotherm of activated **1** at 77 K.

Thermogravimetric analysis (TGA) of as-synthesized **1** exhibited a gradual weight loss of 31.8% between 50 and 365 °C (Figure S1 in the SI), which matched well with the expected

dx.doi.org/10.1021/ja4037516 | J. Am. Chem. Soc. 2013, 135, 8185–8188

loss of 2.2 DMF molecules, including both guest and bound DMF molecules. A second weight loss observed above 400 °C likely corresponds to ligand and framework decomposition. A better-defined TGA trace was obtained when the guest and bound DMF molecules were exchanged with lower-boiling methanol. To achieve this, as-synthesized **1** was subjected to a Soxhlet extraction with freshly dried and deaerated methanol for 2 days, during which the material (methanol-exchanged **1**) acquired a green hue. The replacement of DMF by methanol was tested by IR spectroscopy, which confirmed the absence of the strong DMF C═O stretch at 1647 cm^{-1}, previously prominent in as-synthesized **1**, and the appearance of a methanol C−O stretch at 1005 cm^{-1} (Figure S3). TGA of methanol-exchanged **1** showed a rapid weight loss below ∼100 °C and a stable plateau between 150 and 400 °C (Figure S2). Accordingly, activation of Mn_2(DSBDC) was achieved by heating methanol-exchanged **1** at 150 °C under high vacuum (3 mTorr) for 2 days to obtain activated **1**. The structural integrity of activated **1** was verified by PXRD (Figure 3). The absence of guest and bound methanol was confirmed by IR spectroscopy, and the purity of the sample was confirmed by C, H, and S microanalysis. Upon activation, Mn_2(DSBDC) adsorbed ∼240 cm^3 of N_2/g at 77 K and exhibited a type-I isotherm (Figure 3 inset). The corresponding Brunauer−Emmett−Teller (BET) surface area of 978 m^2/g (329 m^2/mmol) is comparable with those reported for M_2(DOBDC) (287−416 m^2/mmol).[12c,d]

The charge mobilities of methanol-exchanged **1** and activated **1** were evaluated by flash-photolysis time-resolved microwave conductivity (FP-TRMC) measurements. FP-TRMC is a contactless technique that utilizes high-frequency (GHz) microwaves to probe the laser-induced transient conductivity increase, giving information on charge transport on the multi-nanometer length scale. It is particularly informative in measurements of anisotropic crystalline materials because it eliminates perturbations related to grain boundaries, defects, impurities, contact resistance, and high electric fields that can affect the results obtained by the more common direct-current time-of-flight (TOF) and field-effect-transistor measurements, thereby revealing the intrinsic charge mobility of a material.[14] FP-TRMC experiments were performed on films made from poly(methyl methacrylate) and the above two Mn_2(DSBDC) materials, which were mixed in 1:1 weight ratios. The films were inserted into a resonant microwave cavity and irradiated with 355 nm laser light. We obtained time-dependent values of the transient conductivity $\phi\sum\mu$, where ϕ is the quantum efficiency for the generation of charge carriers upon one-photon absorption and $\sum\mu$ is the sum of the electron and hole mobilities. The FP-TRMC profiles of methanol-exchanged and activated **1** were virtually identical, displaying maximum $\phi\sum\mu$ values of 2×10^{-5} cm^2 V^{-1} s^{-1} (Figure 4a). The values of ϕ were estimated by a TOF transient current integration method (Figure 4b). The TOF-derived ϕ values for methanol-exchanged **1** and activated **1** were 9.7×10^{-4} and 1.4×10^{-3}, respectively.

The combination of FP-TRMC and TOF results revealed excellent charge mobilities of 0.02 and 0.01 cm^2 V^{-1} s^{-1} for methanol-exchanged and activated Mn_2(DSBDC), respectively. The similarity between the two values suggests that the charge transport pathway, presumably the Mn−S chain, is not greatly affected by the presence of solvent. On the basis of the observed charge mobility values and the frequency of the microwave field (9.1 GHz), the displacement length of charge carriers (defined as the distance that charge carriers can move in one period of the microwave radiation) in these two Mn_2(DSBDC) materials is 2−

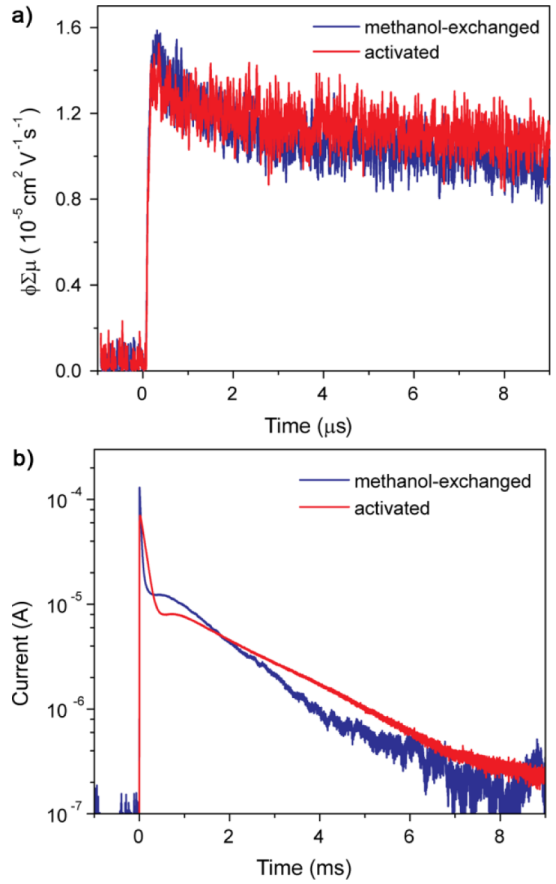

Figure 4. (a) Conductivity transients observed by FP-TRMC upon excitation at 355 nm with 1.4×10^{16} photons/cm^2 per pulse for methanol-exchanged **1** and activated **1**. (b) Photocurrent transients observed by TOF upon excitation at 355 nm with 1.9×10^{14} photons/cm^2 per pulse for methanol-exchanged **1** and activated **1**. The transients were observed with a terminating resistance of 10 kΩ under an applied bias of 3×10^4 V/cm.

3 nm, corresponding to charge delocalization over 8−12 Mn−S units.[15] This short displacement length of charge carriers confirms that the results indeed reveal the intrinsic charge mobility of the materials. As shown in Figure 4b, the photocurrent transients are principally dispersive ones; some inflection points are detectable to give mean flight times of charge carriers (Figure S5). The estimated values of the mobility are 0.001 cm^2 V^{-1} s^{-1} (E = 0 V/cm) according to the TOF results, which are 1 order of magnitude lower than those obtained by FP-TRMC and reflect long-range translational motion of charge carriers. An alternative charge transport pathway may involve transfer through the benzene ring of the 1,4-benzenedithiol moiety.[16] Experiments to probe this possibility are currently underway.

Importantly, the charge mobility values observed for Mn_2(DSBDC) are comparable to those found in organic semiconductors such as polythiophenes ($\sum\mu$ = 0.003−0.1 cm^2 V^{-1} s^{-1})[14a,17] and rubrene ($\sum\mu$ = 0.05 cm^2 V^{-1} s^{-1}),[18] as measured by the same technique, highlighting the potential utility of MOFs for the construction of various electronic devices that combine high surface area and high charge mobility. In fact, at 978 m^2/g, Mn_2(DSBDC) has the highest surface area by almost 50% among MOFs that have demonstrated intrinsic charge delocalization to date, such as Cu[Ni(pyrazine-2,3-dithiolate)$_2$] (385 m^2/g),[3a] Fe(1,2,3-triazolate) (450 m^2/g),[3b]

dx.doi.org/10.1021/ja4037516 | J. Am. Chem. Soc. 2013, 135, 8185−8188

Cu and Ni catecholates (425−490 m^2/g),[3d] and Zn_2(TTF-tetrabenzoate) (662 m^2/g).[3c] Notably, the pore size of the M_2(DOBDC) structure type can be extended into the mesoporous regime;[19] if it is assumed that a similar isoreticular approach is applicable to Mn_2(DSBDC), these results reinforce the idea that high surface area, porosity, and high charge mobility are not mutually exclusive.

In summary, a redox-matching strategy[8] aimed at isomorphous substitution of O atoms by S atoms to yield infinite 1D metal−sulfur chains has led to the synthesis of a new MOF with high charge mobility. Because the isomorphous replacement strategy could be amenable to many other MOFs containing metal−oxygen chains, this study provides a potentially general mechanism for the formation of other porous crystalline materials with high charge mobility, not least of which are members of the M_2(DEBDC) (E = O, S, Se) structure types with other transition metals.

■ ASSOCIATED CONTENT

Ⓢ Supporting Information

Experimental details, table of X-ray refinement details, TGA traces, IR spectra, BET linear fit, TOF data, and crystallographic data (CIF). This material is available free of charge via the Internet at http://pubs.acs.org.

■ AUTHOR INFORMATION

Corresponding Author

mdinca@mit.edu

Notes

The authors declare no competing financial interest.

■ ACKNOWLEDGMENTS

This work was supported by the U.S. Department of Energy, Office of Science, Office of Basic Energy Sciences, under Award DE-SC0006937. The National Science Foundation provided support to the DCIF at MIT (CHE-9808061, DBI-9729592). S.S. was supported by the Funding Program for Next-Generation World-Leading Researchers (NEXT Program) of the Japan Society for the Promotion of Science. We thank Minyuan Li for assistance with the TOC graphic.

■ REFERENCES

(1) Zhou, H.; Long, J. R.; Yaghi, O. M. *Chem. Rev.* **2012**, *112*, 673.

(2) (a) Kreno, L. E.; Leong, K.; Farha, O. K.; Allendorf, M.; Van Duyne, R. P.; Hupp, J. T. *Chem. Rev.* **2012**, *112*, 1105. (b) Hendon, C. H.; Tiana, D.; Walsh, A. *Phys. Chem. Chem. Phys.* **2012**, *14*, 13120.

(3) (a) Kobayashi, Y.; Jacobs, B.; Allendorf, M. D.; Long, J. R. *Chem. Mater.* **2010**, *22*, 4120. (b) Gándara, F.; Uribe-Romo, F. J.; Britt, D. K.; Furukawa, H.; Lei, L.; Cheng, R.; Duan, X.; O'Keeffe, M.; Yaghi, O. M. *Chem.—Eur. J.* **2012**, *18*, 10595. (c) Narayan, T. C.; Miyakai, T.; Seki, S.; Dincă, M. *J. Am. Chem. Soc.* **2012**, *134*, 12932. (d) Hmadeh, M.; Lu, Z.; Liu, Z.; Gándara, F.; Furukawa, H.; Wan, S.; Augustyn, V.; Chang, R.; Liao, L.; Zhou, F.; Perre, E.; Ozolins, V.; Suenaga, K.; Duan, X.; Dunn, B.; Yamamto, Y.; Terasaki, O.; Yaghi, O. M. *Chem. Mater.* **2012**, *24*, 3511.

(4) (a) Kobayashi, A.; Fujiwara, E.; Kobayashi, H. *Chem. Rev.* **2004**, *104*, 5243. (b) Maesato, M.; Kawashima, T.; Furushima, Y.; Saito, G.; Kitagawa, H.; Shirahata, T.; Kibune, M.; Imakubo, T. *J. Am. Chem. Soc.* **2012**, *134*, 17452. (c) Wu, W.; Liu, Y.; Zhu, D. *Chem. Soc. Rev.* **2010**, *39*, 1489. (d) Brooks, J. S. *Chem. Soc. Rev.* **2010**, *39*, 2667.

(5) (a) Heintz, R. A.; Zhao, H.; Ouyang, X.; Grandinetti, G.; Cowen, J.; Dunbar, K. R. *Inorg. Chem.* **1999**, *38*, 144. (b) Avendano, C.; Zhang, Z.; Ota, A.; Zhao, H.; Dunbar, K. R. *Angew. Chem., Int. Ed.* **2011**, *50*, 6543. (c) Zhang, Z.; Zhao, H.; Kojima, H.; Mori, T.; Dunbar, K. R. *Chem.—Eur. J.* **2013**, *19*, 3348. (d) Givaja, G.; Amo-Ochoa, P.; Gómez-García, C.; Zamora, F. *Chem. Soc. Rev.* **2012**, *41*, 115.

(6) (a) Feng, X.; Ding, X.; Jiang, D. *Chem. Soc. Rev.* **2012**, *41*, 6010. (b) Bertrand, G. H. V.; Michaelis, V. K.; Ong, T.-C.; Griffin, R. G.; Dincă, M. *Proc. Nat. Acad. Sci. USA* **2013**, *110*, 4923.

(7) Tranchemontagne, D. J.; Mendoza-Cortés, J. L.; O'Keeffe, M.; Yaghi, O. M. *Chem. Soc. Rev.* **2009**, *38*, 1257.

(8) Holliday, B. J.; Swager, T. M. *Chem. Commun.* **2005**, 23.

(9) (a) Turner, D. L.; Vaid, T. P.; Stephens, P. W.; Stone, K. H.; DiPasquale, A. G.; Rheingold, A. L. *J. Am. Chem. Soc.* **2008**, *130*, 14. (b) Turner, D. L.; Stone, K. H.; Stephens, P. W.; Walsh, A.; Singh, M. P.; Vaid, T. P. *Inorg. Chem.* **2012**, *51*, 370−376.

(10) (a) Xu, Y.; Schoonen, M. A. A. *Am. Mineral.* **2000**, *85*, 543. (b) Makovetskiĭ, G. I.; Galyas, A. I.; Demidenko, O. F.; Yanushkevich, K. I.; Ryabinkina, L. I.; Romanova, O. B. *Phys. Solid State* **2008**, *50*, 1826.

(11) (a) Walsh, A. *Proc. R. Soc. A* **2011**, *467*, 1970. (b) Liu, Y.; Porter, S. H.; Goldberger, J. E. *J. Am. Chem. Soc.* **2012**, *134*, 5044. (c) Li, T.; Liu, Y.-H.; Porter, S.; Goldberger, J. E. *Chem. Mater.* **2013**, *25*, 1477.

(12) (a) Rosi, N. L.; Kim, J.; Eddaoudi, M.; Chen, B.; O'Keeffe, M.; Yaghi, O. M. *J. Am. Chem. Soc.* **2005**, *127*, 1504. (b) Dietzel, P. D. C.; Morita, Y.; Blom, R.; Fjellvåg, H. *Angew. Chem., Int. Ed.* **2005**, *44*, 6354. (c) Wu, H.; Zhou, W.; Yildirim, T. *J. Am. Chem. Soc.* **2009**, *131*, 4995. (d) Bloch, E. D.; Murray, L. J.; Queen, W. L.; Chavan, S.; Maximoff, S. N.; Bigi, J. P.; Krishna, R.; Peterson, V. K.; Grandjean, F.; Long, G. J.; Smit, B.; Bordiga, S.; Brown, C. M.; Long, J. R. *J. Am. Chem. Soc.* **2011**, *133*, 14814.

(13) Vial, L.; Ludlow, R. F.; Leclaire, J.; Pérez-Fernández, R.; Otto, S. *J. Am. Chem. Soc.* **2006**, *128*, 10253.

(14) (a) Saeki, A.; Seki, S.; Sunagawa, T.; Ushida, K.; Tagawa, S. *Philos. Mag.* **2006**, *86*, 1261. (b) Saeki, A.; Koizumi, Y.; Aida, T.; Seki, S. *Acc. Chem. Res.* **2012**, *45*, 1193.

(15) (a) Grozema, F. C.; Siebbeles, L. D. A. In *Charge and Exciton Transport through Molecular Wires*; Siebbeles, L. D. A., Grozema, F. C., Eds.; Wiley-VCH; Weinheim, Germany, 2011; Chapter 9. (b) Amaya, T.; Seki, S.; Moriuchi, T.; Nakamoto, K.; Nakata, T.; Sakane, H.; Saeki, A.; Tagawa, S.; Hirao, T. *J. Am. Chem. Soc.* **2009**, *131*, 408.

(16) Yoshizawa, K. *Acc. Chem. Res.* **2012**, *45*, 1612.

(17) (a) Saeki, A.; Seki, S.; Koizumi, Y.; Sunagawa, T.; Ushida, K.; Tagawa, S. *J. Phys. Chem. B* **2005**, *109*, 10015. (b) Saeki, A.; Ohsaki, S.; Seki, S.; Tagawa, S. *J. Phys. Chem. C* **2008**, *112*, 16643.

(18) Saeki, A.; Seki, S.; Takenobu, T.; Iwasa, Y.; Tagawa, S. *Adv. Mater.* **2008**, *20*, 920.

(19) Deng, H.; Grunder, S.; Cordova, K. E.; Valente, C.; Furukawa, H.; Hmadeh, M.; Gándara, F.; Whalley, A. C.; Liu, Z.; Asahina, S.; Kazumori, H.; O'Keeffe, M.; Terasaki, O.; Stoddart, J. F.; Yaghi, O. M. *Science* **2012**, *336*, 1018.